RESEARCH ARTICLE

The Schlager mouse as a model of altered retinal phenotype

Lakshini Y. Herat[1], Aaron L. Magno[2], Márcio G. Kiuchi[3], Kristy L. Jackson[4], Revathy Carnagarin[3], Geoffrey A. Head[4], Markus P. Schlaich[3, 5, #], Vance B. Matthews[1, *, #]

1 Dobney Hypertension Centre, School of Biomedical Science - Royal Perth Hospital Unit, University of Western Australia, Perth, Australia
2 Research Centre, Royal Perth Hospital, Perth, Australia
3 Dobney Hypertension Centre, School of Medicine - Royal Perth Hospital Unit, University of Western Australia, Perth, Australia
4 Neuropharmacology Laboratory, Baker Heart and Diabetes Institute, Melbourne, Australia
5 Department of Cardiology and Department of Nephrology, Royal Perth Hospital, Perth, Australia

Funding: *The study was generously funded by grants from the Royal Perth Hospital Medical Research Foundation (to VBM and MPS).*

Abstract

Hypertension is a risk factor for a large number of vision-threatening eye disorders. In this study, we investigated for the first time the retinal neural structure of the hypertensive BPH/2J mouse (Schlager mouse) and compared it to its control counterpart, the normotensive BPN/3J strain. The BPH/2J mouse is a selectively inbred mouse strain that develops chronic hypertension due to elevated sympathetic nervous system activity. When compared to the BPN/3J strain, the hypertensive BPH/2J mice showed a complete loss of outer layers of the neural retina at 21 weeks of age, which was indicative of a severe vision-threatening disease potentially caused by hypertension. To elucidate whether the retinal neural phenotype in the BPH/2J strain was attributed to increased BP, we investigated the neural retina of both BPN/3J and BPH/2J mice at 4 weeks of age. Our preliminary results showed for the first time that the BPH/2J strain develops severe retinal neural damage at a young age. Our findings suggest that the retinal phenotype in the BPH/2J mouse is possibly due to elevated blood pressure and may be contributed by an early onset spontaneous mutation which is yet to be identified or a congenital defect occurring in this strain. Further characterization of the BPH/2J mouse strain is likely to i) elucidate gene defects underlying retinal disease; ii) understand mechanisms leading to neural retinal disease and iii) permit testing of molecules for translational research to interfere with the progression of retinal disease. The animal experiments were performed with the approval of the Royal Perth Hospital Animal Ethics Committee (R535/17-18) on June 1, 2017.

Key Words: *blood pressure; eye; hypertension; mice; neural regeneration; retina; Schlager mouse; sympathetic nervous system*

Chinese Library Classification No. *R459.9; R364; R774*

Correspondence to:
Vance B. Matthews, PhD,
vance.matthews@uwa.edu.au.

#Both authors contributed equally to this paper.

orcid:
0000-0001-9804-9344
(Vance B. Matthews)

doi: *10.4103/1673-5374.266069*

Received: *May 23, 2019*
Accepted: *August 5, 2019*

Introduction

High blood pressure (or hypertension) is a condition of the circulatory system affecting over 1.3 billion individuals and it poses a significant public health challenge worldwide (Mills et al., 2016). An increase in systemic blood pressure (BP) alters retinal blood flow through impaired autoregulation and hyper-perfusion has a profound effect on the structure and function of the eye (van Koeverden et al., 2018). The retinal, choroidal, and optic nerve circulation can undergo a series of pathophysiological changes in response to raised BP, leading to a broad range of clinical symptoms referred to as hypertensive retinopathy, hypertensive choroidopathy and hypertensive optic neuropathy. Furthermore, elevated BP is an important risk factor for the development of diabetic retinopathy, glaucoma, age-related macular degeneration and retinal vein and artery occlusion (Wong and Mitchell, 2007; Fraser-Bell et al., 2017).

In particular, hypertensive retinopathy (HR) is a progressive disease characterized by a spectrum of retinal vascular and neural alterations in people with elevated BP. The prevalence of HR increases with severity of BP elevation and is a predictor of cardiovascular outcomes (Grosso et al., 2005). In the retina, with increased blood pressure, the blood-retinal barrier is compromised, resulting in hemorrhages, lipid exudates also known as hard exudates, and subsequent ischemia of nerve-fiber layers (cotton-wool spots) (Grosso et al., 2005; Fraser-Bell et al., 2017). In the setting of further elevation of high blood pressure, raised intracranial pressure and associated optic nerve ischemia can lead to optic disc swelling or hypertensive optic neuropathy (Wong and Mitchell, 2007). Alterations in retinal blood flow in HR leads to inflammation (Klein et al., 2000), endothelial dysfunction (Klein et al., 2000; Delles et al., 2004) and angiogenesis due to upregulation of well-known growth factors such as vascular endothelial growth factor (VEGF) and its receptor VEGF-R2 (Suzuma et al., 2001; Tsai et al., 2005).

A recent conceptual advancement in HR is the recognition that it is also a disease of the neurovascular unit, with multiple, interdependent cell types contributing to the dysfunction of the retina, as demonstrated in angiotensin II-induced hypertensive double transgenic rats (Reichhart et al., 2016). New therapeutic approaches should therefore adopt a more holistic view of how hypertension affects the retina and tailor appropriate treatments to more precisely define disease

phenotypes with the prospect of achieving better clinical outcomes. However, to date a suitable mouse model of hypertensive retinopathy does not exist. Our study is the first to examine the BPH/2J genetic model of hypertension for its ocular phenotype. This strain was selectively bred in 1964 by the Jacksons Laboratory using a two-way selection process (https://www.jax.org/strain/003005). The BPH/2J strain exhibited elevated BP compared to the hypotensive (BPL/1J) and normotensive (BPN/3J) controls that were bred in parallel. Whilst originally bred to evaluate the genetics of hypertension, this strain is currently being studied in a wide range of areas (Jackson et al., 2018; Watson et al., 2019).

Characterization of a true hypertensive mouse model for its ocular phenotype would provide an important pre-clinical resource for the study of HR found in patients. In this study, we tested the hypothesis that hypertension in the BPH/2J strain may lead to the progressive development of HR in the BPH/2J mouse.

Materials and Methods

Experiments were carried out on 4-, 6-, 13-, 17-, or 21-week-old BPN/3J and BPH/2J mice of both genders and maintained in specific pathogen-free conditions at the Animal Resources Centre, Perth, Western Australia. At 13 weeks of age, male and female mice were greater than 19 and 16 g respectively. During the full duration of the experiment, mice were maintained under a 12-hour light/dark cycle, with free access to a standard chow diet and acidified water at the Royal Perth Hospital Animal Holding Facility.

The animal experiments were performed with the approval of the Royal Perth Hospital Animal Ethics Committee (R535/17-18) on June 1, 2017 and in accordance with the Association for Research in Vision and Ophthalmology statement for the Use of Animals in Ophthalmic and Vision Research.

Measurement of blood pressure

All animals undergoing BP analysis were acclimatized for a period of 7 days. The BP measurements were conducted at 6 (n = 5) and 13 weeks (n = 11) in BPN/3J mice and 6 (n = 5) and 13 weeks (n = 14) in BPH/2J mice. Time-course BP measurements were carried out only on BPH/2J (n = 14) mice at 17 and 21 weeks.

A non-invasive computer automated multi-channel BP analysis system (MC4000, Hatteras Instruments, Cary, NC, USA) was used for the rapid evaluation of BPs. The mouse was placed on a 37.7°C metal platform surface and restrained in a holder (3 cm wide, 3.3 cm high) with free access to the tail. The tail was threaded through the occlusion cuff (13 mm long, 9 mm diameter) and positioned in the "v-notch" sensory assembly and immobilized with adhesive tape. The sensory assembly was equipped with an optical path with a LED light source above and a photosensor below the tail. The blood pulse wave in the tail artery is detected as transformed into an optical pulse signal by measurement of light extinction. Pulse detection, cuff inflation and pressure evaluation were automated by the SC1000 Comm software (Hatteras Instruments). Each recording session consisted of 20 inflation and deflation cycles per set, of which the first five cycles were "acclimation" cycles and were not used in the analysis, whereas the following 15 cycles were used for obtaining systolic blood pressure (SBP), diastolic blood pressure (DBP) and mean arterial pressure (MAP). Measurement cycles with movement artefacts were excluded. The SBP indicates the pressure of circulating blood due to the heart pumping blood through the circulatory system; DBP indicates the pressure during ventricular relaxation where the cardiac ventricles refill with blood and MAP indicates the average pressure in the arteries during one cardiac cycle. All measurements were made in the morning (9:00–11:30 a.m.).

Eye specimen collection, section preparation and histological analysis

At the experimental end-point of 4 weeks (BPN/3J, n = 3 and BPH/2J, n = 6) or 21 weeks (BPN/3J, n = 3 and BPH/2J, n = 4) of age, animals were euthanized by methoxyflurane inhalation followed by cervical dislocation. Eyes were enucleated, cleaned and collected into 10% buffered formalin for histology. Upon fixation for 24 hours at room temperature, eyes were placed in 70% ethanol overnight followed by wax embedding in sagittal orientation (optic nerve parallel to cassette surface). Tissue blocks were trimmed for excess paraffin and sections were cut at 5 μm thickness using a Leica semi-automated RM2245 microtome (Leica Biosystems, Sydney, Australia) and placed in a 33°C water bath. Sections were aligned and collected onto super-frost slides. Each slide contained six sections. All slides were air dried overnight followed by oven drying at 60°C for 3 hours. Sections were deparaffinized in two changes of xylene, rehydrated in one change of absolute alcohol and 95% alcohol followed by 70% alcohol. Slides were then placed under running water followed by staining the nuclei with Gill's hematoxylin (Sigma, Sydney, Australia) and placed again under running water. Acid alcohol at 1% was used for differentiation. Slides were then placed in bluing Scott's water and washed in mild warm water, then dipped in 95% ethanol followed by treatment with alcoholic eosin (Sigma). Rapid dehydration in a series of ethanol (95% and 100% ethanol) followed by clearing twice in xylene and finally mounted using dibutylphthalate polystyrene xylene (DPX) (Sigma). Hematoxylin & eosin-stained retinal sections were visualized and imaged using the inverted microscopic systems Nikon Eclipse Ti (Nikon, Tokyo, Japan) equipped with a digital camera (CoolSNAP HQ2, Photometrics, Tucson, AZ, USA) linked to a computer running image analysis software NIS-Elements Advanced Research (Nikon). Morphometric measurements were obtained for retinal layer thickness of the full neural retina and individual retinal layers from the mid retinal region (4 weeks: BPN/3J, n = 3 and BPH/2J, n = 3 and 21 weeks: BPN/3J, n = 3 and BPH/2J, n = 3).

Cell death detection using TUNEL assay

Tissue sections from 4-week-old BPH/2J (n = 3) were processed for the identification of apoptosis by terminal deoxy-

nucleotidyl transferase-mediated dUTP nick-end labeling (TUNEL) according to the manufacturer's instructions (In Situ Cell Death Detection Kit, POD, Roche Applied Science, Bavaria, Germany). In brief, the sections were dewaxed, and rehydrated through a graded series of ethanol and rinsed in distilled water as stated above. Sections underwent antigen retrieval in ethylenediaminetetraacetic acid (EDTA) pH 8.5 (Sigma) followed by three washes in phosphate buffer saline (PBS). Positive controls were treated with 2370 U/mL of DNase I mixed in 50 mM Tris-HCl (pH 7.5), and 1mg/mL bovine serum albumin for 10 minutes at room temperature. All slides were incubated with 3% H_2O_2 for 10 minutes before washes with PBS. Sections were incubated with 50 µL of TUNEL reaction mixture containing both terminal deoxynucleotidyl transferase (TdT) and label solution, while corresponding negative controls were incubated only with the label solution for 60 minutes at 37°C in a humidified chamber. Following washes with PBS, each section was incubated with 50 µL of Converter-POD for 30 minutes at 37°C in a humidified chamber. Slides were washed in PBS and 50 µL of 3, 3′-diaminobenzidine substrate was added to each section. DNase I treated sections were washed in PBS after 20 seconds, while all other sections were washed in PBS after 10 minutes. Slides were mounted using DPX (Sigma) followed by visualization and imaging as described above for histological analysis.

Statistical analysis

All cardiovascular data are expressed as mean ± SEM. Data were compared using a two-tailed Student's *t*-test or one-way analysis of variance test where applicable. All analysis and graphs were generated using GraphPad Prism 7 (GraphPad Software Inc., La Jolla, California, USA). The data were deemed significant when $P < 0.05$.

Results

Blood pressure measurements in BPN/3J and BPH/2J mice

Our tail-cuff BP analysis showed that at 13 weeks of age SBP, DBP and MAP were greater in hypertensive BPH/2J mice when compared to the normotensive BPN/3J mice ($P < 0.01$; **Figure 1**). **Figure 2** shows that even at 6 weeks of age, the SBP, DBP and MAP were significantly greater ($P < 0.01$) in the BPH/2J mice when compared to BPN/3J mice. In BPH/2J mice, BP was measured every 4 weeks starting at 13 weeks until 21 weeks of age. A mild increase in BP was noted at 17 weeks of age but by 21 weeks of age, DBP and MAP were similar to that of 13-week-old mice (**Figure 3**).

Retinal neural architecture BPN/3J and BPH/2J mice

At 21 weeks of age, BPN/3J eyes showed the normal neural structure of the retina whereby all eight retinal layers were visible (**Figure 4A** and **C**). In contrast, the BPH/2J strain showed an overall thinner neural structure (**Figure 4B** and **D**) with only five retinal layers (**Figure 4D**). The BPH/2J retina was devoid of outer plexiform, outer nuclear and photoreceptor layers (**Figure 4D**).

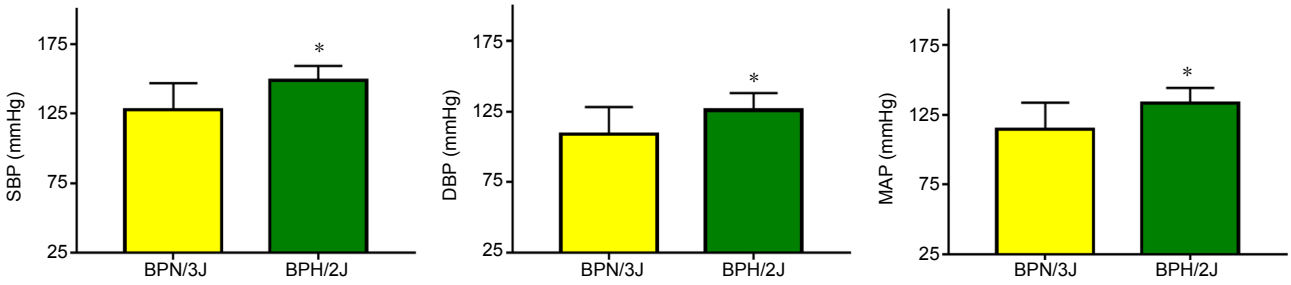

Figure 1 Tail-cuff blood pressure measurements in 13-week-old BPN/3J and BPH/2J mice.
In comparison to BPN/3J ($n = 11$) mice, BPH/2J ($n = 14$) mice showed significantly higher systolic, diastolic and mean arterial pressure respectively. DBP: Diastolic blood pressure; MAP: mean arterial pressure; SBP: systolic blood pressure. Data are presented as mean ± SEM; $*P < 0.01$, *vs.* BPN/3J mice (Student's *t*-test).

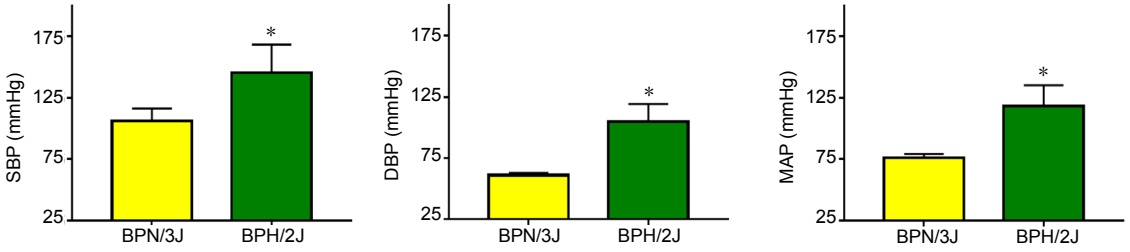

Figure 2 Tail-cuff blood pressure measurements in 6-week-old BPN/3J and BPH/2J mice.
In comparison to BPN/3J ($n = 5$) mice, BPH/2J ($n = 5$) mice showed significantly higher systolic, diastolic and mean arterial pressure respectively. DBP: Diastolic blood pressure; MAP: mean arterial pressure; SBP: systolic blood pressure. Data are presented as mean ± SEM; $*P < 0.01$, *vs.* BPN/3J mice (Student's *t*-test).

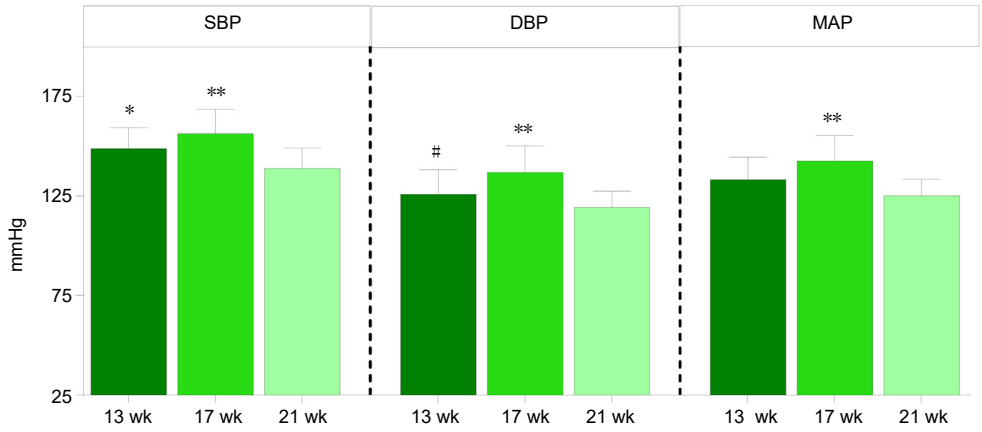

Figure 3 Tail-cuff blood pressure measurements in BPH/2J mice at 13, 17 and 21 weeks of age.
Averaged data showing SBP, DBP and MAP measured every 4 weeks in BPH/2J (n = 14) mice starting at 13 weeks of age. Data are presented as mean ± SEM. $*P < 0.05$, $**P < 0.01$, *vs.* 21 weeks; $\#P < 0.05$, *vs.* 17 weeks (one-way analysis of variance). DBP: Diastolic blood pressure; MAP: mean arterial pressure; SBP: systolic blood pressure.

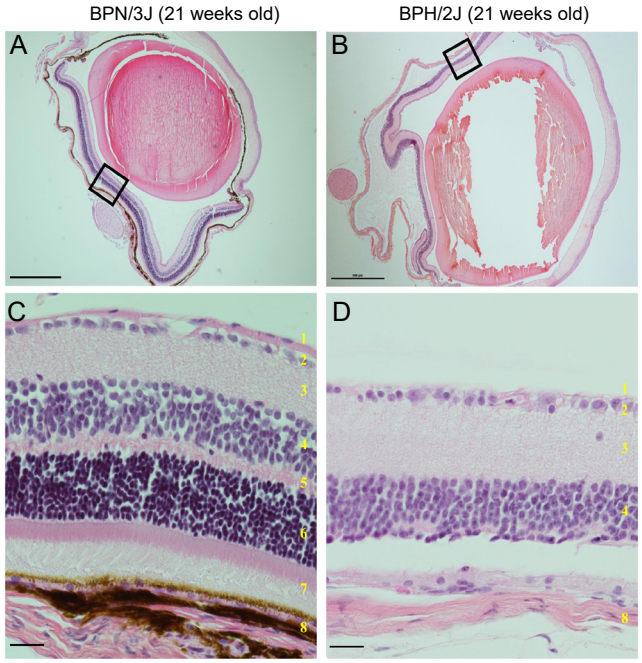

Figure 4 Phenotype of the neural retina in adult BPN/3J and BPH/2J mice.
Sectioned full eye stained with hematoxylin and eosin of BPN/3J (A) and BPH/2J (B) mice at 21 weeks of age. Higher magnification of the BPN/3J retina showing all eight layers of the neural retina (C) whereas the BPH/2J Schlager mouse shows reduced retinal depth due to the lack of the outer plexiform, outer nuclear and photoreceptor layers (D). Black boxes in A and B: higher magnification region, 1: Nerve fiber layer, 2: ganglion cell layer, 3: inner plexiform layer, 4: inner nuclear layer, 5: outer plexiform layer, 6: outer nuclear layer, 7: photoreceptor layer and 8: choroid. Scale bars: 500 µm in A and B, 100 µm in C and D. Images are representative of n = 3–4 mice/strain.

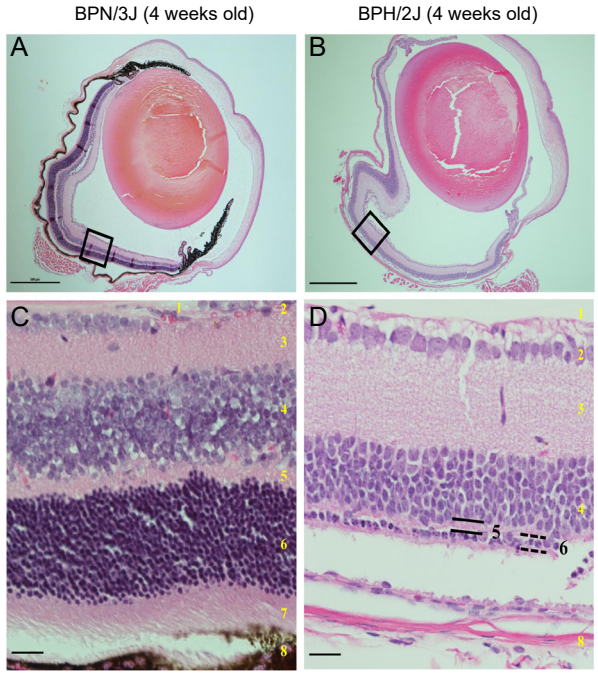

Figure 5 Phenotype of the neural retina in young BPN/3J and BPH/2J mice.
Sectioned full eye stained with haematoxylin and eosin of BPN/3J (A) and BPH/2J (B) mice at 4 weeks of age. Higher magnification of the BPN/3J retina showing all eight layers of the neural retina (C) whereas the BPH/2J Schlager mouse shows reduced retinal depth (D) due to markedly reduced outer plexiform (D; black numeric 5 and continuous line) and outer nuclear (D; black numeric 6 and dash line) layers and the complete lack of the photoreceptor layer. Black boxes in A and B: higher magnification region, 1: Nerve fiber layer, 2: ganglion cell layer, 3: inner plexiform layer, 4: inner nuclear layer, 5: outer plexiform layer, 6: outer nuclear layer, 7: photoreceptor layer and 8: choroid. Scale bars: 500 µm in A and B, 100 µm in C and D. Images are representative of n = 3–4 mice/strain.

It was evident that at 4 weeks of age, the BPH/2J retina appeared thinner (**Figure 5B** and **D**) when compared to the normal retina of the BPN/3J (**Figure 5A** and **C**). At 4 weeks of age, the BPH/2J retina showed the presence of significantly thinner outer plexiform and outer nuclear layers (**Additional Figure 1A**) when compared to the BPN/3J retina (**Additional Figure 1B**). However, the rod and cone cells and cell bodies showed complete absence (**Figure 5D**), similar to that of 21 week old BPH/2J mice (**Figure 4D**).

Retinal layer thickness in BPN/3J and BPH/2J mice

Upon retinal layer thickness measurement, it was noted that the overall retina was significantly thicker in BPN/3J mice when compared to BPH/2J mice at 4 (**Figure 6**) and

21 weeks of age (**Figure 6**). We then compared the thickness of each layer between 4 week old BPN/3J and BPH/2J mice. In this group, the outer plexiform layer (OPL; $P = 0.03$) and outer nuclear layer (ONL; $P = 0.0001$) was significantly thinner in the BPH/2J mice (**Figure 7**). In 21-week-old BPN/3J and BPH/2J mice, the comparison of retinal layer thickness showed absence of the OPL and ONL in the BPH/2J mice (**Figure 7**).

In BPH/2J mice (**Figure 7B**), the inner nuclear layer in 4-week-old mice was significantly thinner compared to 21 week old BPH/2J mice ($P = 0.02$). Furthermore, 4-week-old BPH/2J mice showed limited presence of the OPL and ONL when compared to the BPH/2J mice at 21 weeks of age, where complete loss of OPL and ONL was evident. In both 4- and 21-week-old BPH/2J mice, the photoreceptor layer was absent (**Figure 7B**).

Apoptosis in retinal cells of young BPH/2J mice

A marker for apoptosis is TUNEL staining, which demonstrates nuclear DNA fragmentation in cells progressing towards cell death. It is a common phenomenon seen in retinal degeneration in both mice (Portera-Cailliau et al., 1994) and in humans (Li and Milam, 1995). In 4-week-old BPH/2J mice, TUNEL-positive cells were occasionally noted only in the retinal ganglion cell layer (**Figure 8**).

Discussion

The BPH/2J mouse strain is a genetic model of hypertension (Marques et al., 2011) which was selectively bred to achieve elevated blood pressure alongside their normotensive (BPN/3J) control counterparts (Schlager, 1994). Recent studies have shown that the hypertension in the BPH/2J strain is caused by enhanced activation of the sympathetic nervous system since ganglion blockade leads to a greater depressor response in BPH/2J mice compared with BPN/3J controls (Davern et al., 2009; Jackson et al., 2013). The hypertensive BPH/2J mice have shown elevated SBP (~36 mmHg greater at 4–21 weeks of age) when compared to the normotensive BPN/3J strain (Schlager and Sides, 1997). The present study confirms previous findings that the BPH/2J mice are hypertensive when compared to BPN/3J mice at an early age such as 6 weeks of age and the BPH/2J mice consistently maintained the hypertensive status until 21 weeks of age (Schlager and Sides, 1997; Jackson et al., 2016). Although the time point 4 weeks was not investigated in this study due to technical feasibility of the tail-cuff BP method (Marques et al., 2011), it is highly unlikely that the BPH/2J mice are normotensive at 4 weeks of age. It is likely that the BP surge seen in the BPH/2J mice at 6 weeks of age also existed at 4 weeks of age.

Hypertension is a potential risk factor for several ocular diseases such as hypertensive retinopathy, age-related macular degeneration and glaucoma and these conditions can lead to compromised retinal vascular and neural structure. Given the hypertensive phenotype in the BPH/2J mouse, we assessed the retinal neural structure anticipating observing lesions indicative of hypertension driven ocular disease. To our knowledge, this study is the first to evaluate the eye phenotype in the BPH/2J hypertensive mouse, a model that exhibits a BP surge as observed in humans with hypertension. At 21 weeks of age, the eyes of the BPH/2J mouse showed severe retinal neural damage compared to the control counterparts, BPN/3J. As previously reported in other mouse strains, severe retinal damage caused to the outer layers of the retina is responsible for vision impairment (Won et al., 2011; Chang, 2013). Furthermore, the retinal neural phenotype seen in the BPH/2J mice at 21 weeks of age may represent the retinal phenotype seen in humans and mouse models of retinal disease (Chang et al., 2002; Veleri et al., 2015). However, given the known hypertensive background of the BPH/2J strain, one possible notion was that the elevated BP pattern in these mice may lead to progressive neural damage of the retina and possibly blindness. Therefore, we then set out to establish whether severe retinal neural damage in the BPH/2J strain may be attributed to an increase in BP. To achieve this, we investigated the neural retina of 4-week-old BPN/3J and BPH/2J mice. Our findings showed that in young BPH/2J mice, the neural retina was completely lacking the photoreceptor layer and the OPL and ONL were minimally present. At this young age, BPH/2J mice could be hypertensive (Schlager and Sides, 1997) and this may have contributed to the retinal neural damage seen in the BPH/2J mice. The extensively altered retinal phenotype in the BPH/2J strain is highly unlikely to be caused primarily due to the elevation of BP and it is entirely possible that the neural damage of the retina in this model could be the outcome of a genetic mutation or congenital defect. However, it is plausible that the elevated BP levels may have exacerbated the process of retinal damage in these mice. Therefore, our study has identified for the first time, a hypertensive mouse model with end-stage retinal neural damage possibly caused by a genetic mutation or congenital defect where the retinal damage process may have worsened by the elevated BP.

Genome-wide association studies conducted between BPN/3J and BPH/2J mice have identified genes altered in the early and established phases of hypertension (Marques et al., 2011). Of the identified genes, Atp2b1 (plasma membrane calcium-transporting ATPase 1) is of particular interest as ATP2B1 plays important roles in the regulation of blood pressure through alteration of calcium handling and vasoconstriction in vascular smooth muscle cells (Kobayashi et al., 2012). It is shown that plasma membrane calcium-transporting ATPase (PMCA) isoforms could play a specific functional role in the development of the mammalian retina. In particular, plasma membrane calcium-transporting ATPase 1 which is predominantly expressed in photoreceptors, cone bipolar cells and possibly horizontal cells, is shown to be of importance for the maintenance of normal photoreceptor cell function and signaling (Krizaj et al., 2002).

Numerous serious or disabling eye diseases such as age-related macular degeneration, retinitis pigmentosa and glaucoma in humans affect millions of individuals world-wide (Johnson et al., 1999). Mouse models of abnormal ocular phenotypes provide powerful tools for i) the identification of potential genetic markers of ocular disease and ii) allow

possible testing of therapeutic interventions. Studies conducted on mouse models with altered retinal phenotypes are important to understand the pathophysiology, as well as the etiology of similar human ocular diseases.

It is noteworthy that spontaneous mutations leading to severe retinal neural damage occur in a wide variety of murine strains (Won et al., 2011; Chang, 2013). However, the observation of altered phenotypes in mice of different genetic backgrounds can provide means for the identification of interacting genes and molecular pathways involved in the pathophysiology of a broad range of ocular diseases. This could be essential for the discovery of potential therapeutic targets as interventions for retinal neural damage. Further investigations in the BPH/2J strain should be of priority to identify potential genetic mutations which may possibly be responsible for the very early (~4 weeks) retinal neural damage. This could lead to the discovery of genetic defects similar to that of human retinal neural damage (Won et al., 2011). The availability of experimental animals with similar genetic defects to humans with retinal neural damage, such as in retinitis pigmentosa, will assist with the development of suitable therapeutic approaches.

Future investigations will enable the full characterization of the retinal phenotype of the BPH/2J strain which can then be used to test therapeutics which will promote the development of neural retinal layers. A promising future approach could be the transplantation of healthy retinal photoreceptors which will aid the restoration of appropriate connections with inner retinal neurons (Gouras et al., 1992; Kwan et al., 1999).

Author contributions: *LYH performed experiments and prepared the manuscript. ALM performed experiments and assisted with manuscript preparation. MGK assisted with manuscript preparation. KLJ performed experiments. RC and GAH assisted with manuscript preparation. MPS assisted with manuscript preparation and obtained the funding. VBM performed experiments, assisted with manuscript preparation and obtained the funding. All authors approved the final manuscript.*
Conflicts of interest: *None declared.*
Financial support: *The study was generously funded by grants from the Royal Perth Hospital Medical Research Foundation (to VBM and MPS).*
Institutional review board statement: *The animal experiments were performed with the approval of the Royal Perth Hospital Animal Ethics Committee (R535/17-18) on June 1, 2017 and in accordance with the Association for Research in Vision and Ophthalmology statement for the Use of Animals in Ophthalmic and Vision Research.*

Data sharing statement: *Datasets analyzed during the current study are available from the corresponding author on reasonable request.*
Plagiarism check: *Checked twice by iThenticate.*
Peer review: *Externally peer reviewed.*

Additional file:
Additional Figure 1: *Histological sections from BPH/2J young and old mice showing progressive loss of outer retinal layers.*

References

Chang B (2013) Mouse models for studies of retinal degeneration and diseases. Methods Mol Biol 935:27-39.
Chang B, Hawes NL, Hurd RE, Davisson MT, Nusinowitz S, Heckenlively JR (2002) Retinal degeneration mutants in the mouse. Vision Res 42:517-525.
Davern PJ, Nguyen-Huu TP, La Greca L, Abdelkader A, Head GA (2009) Role of the sympathetic nervous system in Schlager genetically hypertensive mice. Hypertension 54:852-859.
Delles C, Michelson G, Harazny J, Oehmer S, Hilgers KF, Schmieder RE (2004) Impaired endothelial function of the retinal vasculature in hypertensive patients. Stroke 35:1289-1293.
Fraser-Bell S, Symes R, Vaze A (2017) Hypertensive eye disease: a review. Clin Exp Ophthalmol 45:45-53.
Gouras P, Du J, Kjeldbye H, Yamamoto S, Zack DJ (1992) Reconstruction of degenerate rd mouse retina by transplantation of transgenic photoreceptors. Invest Ophthalmol Vis Sci 33:2579-2586.
Grosso A, Veglio F, Porta M, Grignolo FM, Wong TY (2005) Hypertensive retinopathy revisited: some answers, more questions. Br J Ophthalmol 89:1646-1654.
Jackson KL, Dampney BW, Moretti JL, Stevenson ER, Davern PJ, Carrive P, Head GA (2016) Contribution of Orexin to the Neurogenic Hypertension in BPH/2J Mice. Hypertension 67:959-969.
Jackson KL, Marques FZ, Lim K, Davern PJ, Head GA (2018) Circadian Differences in the contribution of the brain renin-angiotensin system in genetically hypertensive mice. Front Physiol 9:231.
Jackson KL, Marques FZ, Watson AM, Palma-Rigo K, Nguyen-Huu TP, Morris BJ, Charchar FJ, Davern PJ, Head GA (2013) A novel interaction between sympathetic overactivity and aberrant regulation of renin by miR-181a in BPH/2J genetically hypertensive mice. Hypertension 62:775-781.
Johnson JG, Minassian DC, Weale R (1999) The epidemiology of eye disease. Community Eye Health 12:10.
Klein R, Sharrett AR, Klein BE, Chambless LE, Cooper LS, Hubbard LD, Evans G (2000) Are retinal arteriolar abnormalities related to atherosclerosis?: The Atherosclerosis Risk in Communities Study. Arterioscler Thromb Vasc Biol 20:1644-1650.
Kobayashi Y, Hirawa N, Tabara Y, Muraoka H, Fujita M, Miyazaki N, Fujiwara A, Ichikawa Y, Yamamoto Y, Ichihara N, Saka S, Wakui H, Yoshida S, Yatsu K, Toya Y, Yasuda G, Kohara K, Kita Y, Takei K, Goshima Y, et al. (2012) Mice lacking hypertension candidate gene ATP2B1 in vascular smooth muscle cells show significant blood pressure elevation. Hypertension 59:854-860.
Krizaj D, Demarco SJ, Johnson J, Strehler EE, Copenhagen DR (2002) Cell-specific expression of plasma membrane calcium ATPase isoforms in retinal neurons. J Comp Neurol 451:1-21.
Kwan AS, Wang S, Lund RD (1999) Photoreceptor layer reconstruction in a rodent model of retinal degeneration. Exp Neurol 159:21-33.
Li ZY, Milam AH (1995) Apoptosis in Retinitis Pigmentosa. In: Degenerative Diseases of the Retina (Anderson RE, LaVail MM, Hollyfield JG, eds), pp 1-8. Boston, MA: Springer.
Marques FZ, Campain AE, Davern PJ, Yang YH, Head GA, Morris BJ (2011) Global identification of the genes and pathways differentially expressed in hypothalamus in early and established neurogenic hypertension. Physiol Genomics 43:766-771.
Mills KT, Bundy JD, Kelly TN, Reed JE, Kearney PM, Reynolds K, Chen J, He J (2016) Global disparities of hypertension prevalence and control: a systematic analysis of population-based studies from 90 countries. Circulation 134:441-450.
Portera-Cailliau C, Sung CH, Nathans J, Adler R (1994) Apoptotic photoreceptor cell death in mouse models of retinitis pigmentosa. Proc Natl Acad Sci U S A 91:974-978.
Reichhart N, Haase N, Crespo-Garcia S, Skosyrski S, Herrspiegel C, Kociok N, Fuchshofer R, Dillinger A, Poglitsch M, Muller DN, Joussen AM, Luft FC, Dechend R, Strauß O (2016) Hypertensive retinopathy in a transgenic angiotensin-based model. Clin Sci (Lond) 130:1075-1088.
Schlager G (1994) Biometrical genetic analysis of blood pressure level in the genetically hypertensive mouse. Clin Exp Hypertens 16:809-824.
Schlager G, Sides J (1997) Characterization of hypertensive and hypotensive inbred strains of mice. Lab Anim Sci 47:288-292.
Suzuma I, Hata Y, Clermont A, Pokras F, Rook SL, Suzuma K, Feener EP, Aiello LP (2001) Cyclic stretch and hypertension induce retinal expression of vascular endothelial growth factor and vascular endothelial growth factor receptor-2: potential mechanisms for exacerbation of diabetic retinopathy by hypertension. Diabetes 50:444-454.
Tsai WC, Li YH, Huang YY, Lin CC, Chao TH, Chen JH (2005) Plasma vascular endothelial growth factor as a marker for early vascular damage in hypertension. Clin Sci (Lond) 109:39-43.
van Koeverden AK, He Z, Nguyen CTO, Vingrys AJ, Bui BV (2018) Systemic hypertension is not protective against chronic intraocular pressure elevation in a rodent model. Sci Rep 8:7107.
Veleri S, Lazar CH, Chang B, Sieving PA, Banin E, Swaroop A (2015) Biology and therapy of inherited retinal degenerative disease: insights from mouse models. Dis Model Mech 8:109-129.
Watson AMD, Gould EAM, Penfold SA, Lambert GW, Pratama PR, Dai A, Gray SP, Head GA, Jandeleit-Dahm KA (2019) Diabetes and hypertension differentially affect renal catecholamines and renal reactive oxygen species. Front Physiol 10:309.
Won J, Shi LY, Hicks W, Wang J, Hurd R, Naggert JK, Chang B, Nishina PM (2011) Mouse model resources for vision research. J Ophthalmol 2011:391384.
Wong TY, Mitchell P (2007) The eye in hypertension. Lancet 369:425-435.

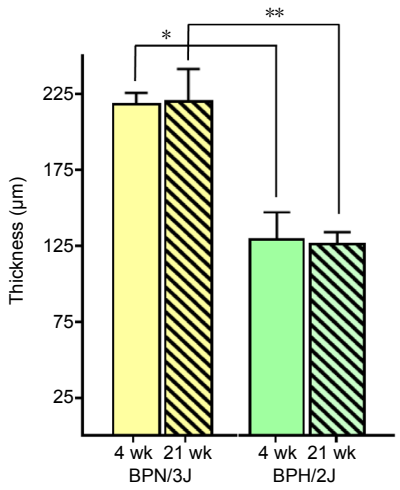

Figure 6 Total retinal layer thickness in young and adult BPN/3J and BPH/2J mice.
Retinal sections from BPN/3J and BPH/2J mice at 4 and 21 weeks were stained with hematoxylin and eosin. Quantitative measurement of total retinal thickness showed a significant decrease in BPH/2J mice compared to BPN/3J mice at 4 and 21 weeks of age. Data are presented as the mean ± SEM; ∗ and ∗∗$P \leq 0.0001$ (Student's *t*-test). $n = 3$ mice/group.

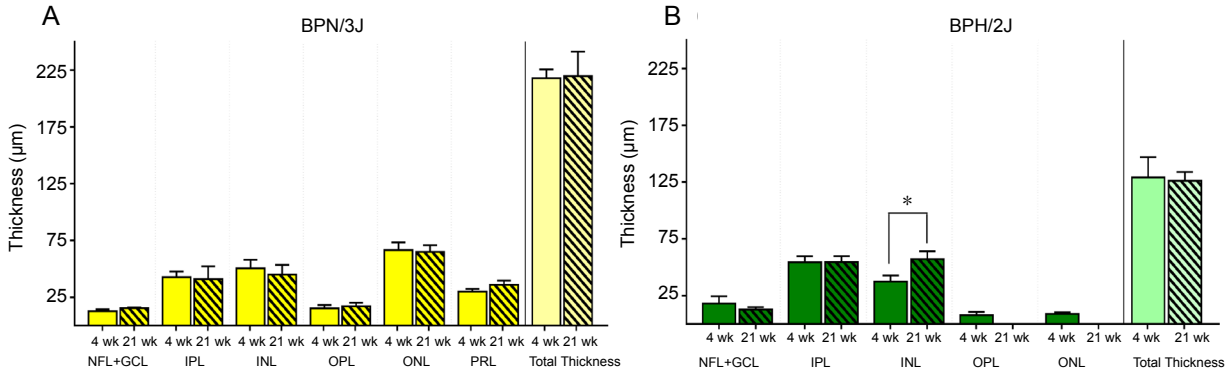

Figure 7 Retinal layer thickness in young and adult BPN/3J and BPH/2J mice.
Retinal sections from BPN/3J (A) and BPH/2J (B) mice at 4 and 21 weeks of age were stained with haematoxylin and eosin. Quantitative measures of retinal layer thickness in BPH/2J show that by 21 weeks of age, the OPL and ONL were completely ablated. GCL: Ganglion cell layer; INL: inner nuclear layer; IPL: inner plexiform layer; NFL: Nerve fiber layer; ONL: outer nuclear layer; OPL: outer plexiform layer; PRL: photoreceptor layer. Data are presented as the mean ± SEM; ∗$P < 0.05$ (Student's *t*-test). $n = 3$ mice/group.

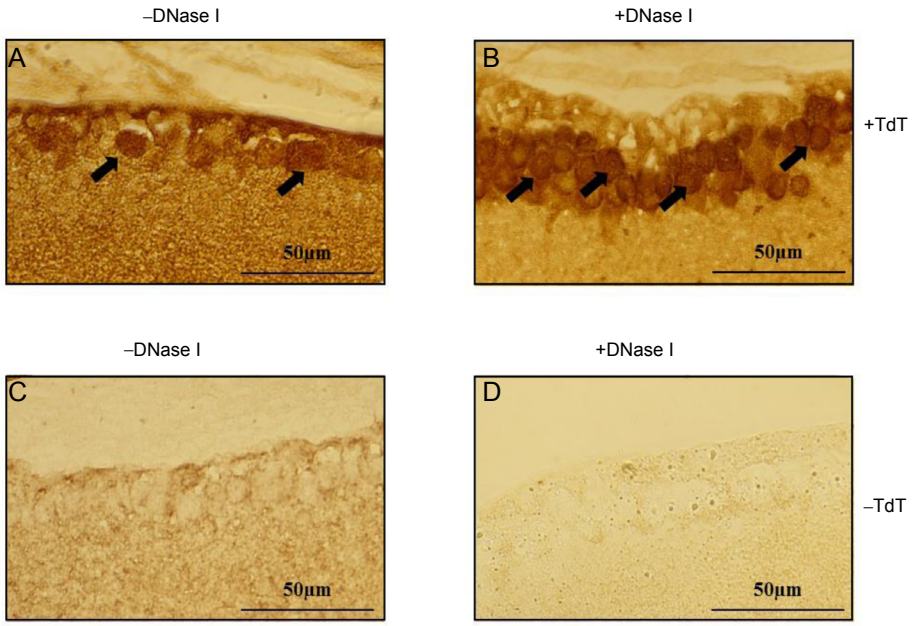

Figure 8 Cell death detection in the retina of 4-week-old BPH/2J Schlager mice.
Representative images of TUNEL staining in the retinal ganglion cell layer of BPH/2J mice ($n = 3$). Samples not treated with DNase I (A and C) were exposed to 3,3′-diaminobenzidine for 10 minutes while the DNase I treated (B and D) were exposed to substrate for 20 seconds. Scale bars: 50 µm. Arrows indicate TUNEL positive nuclei. TdT: Terminal deoxynucleotidyl transferase; TUNEL: terminal deoxynucleotidyl transferase-mediated dUTP nick-end labeling.

C-Editors: Zhao M, Li CH; T-Editor: Jia Y

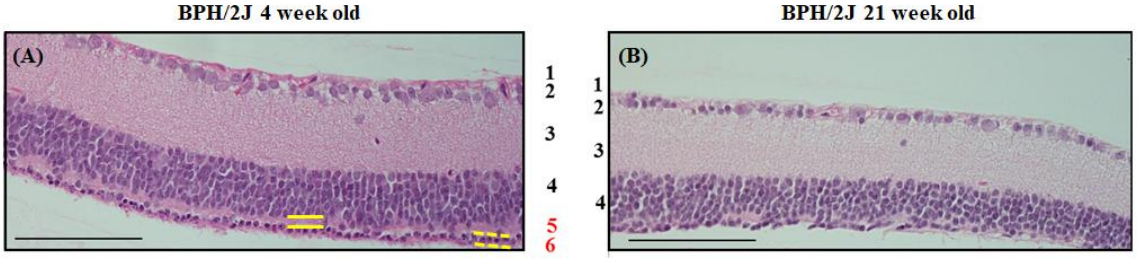

Additional Figure 1 Histological sections from BPH/2J young and old mice showing progressive loss of outer retinal layers.

At 4 weeks of age (A) thinning of outer plexiform (A: red number 5 and continuous yellow lines) and outer nuclear (A: red number 6 and dashed yellow lines) layers were noted while at 21 weeks of age (B) complete absence of outer plexiform and out nuclear layers were noted. 1: Nerve fiber layer, 2: ganglion cell layer, 3: inner plexiform layer, 4: inner nuclear layer, 5: outer plexiform layer and 6: outer nuclear layer. Scale bars: 100 µm. Images are representative of $n = 3$ mice/time point.